Stability of an anthropomorphic multimodality (CT/MRI) head and neck phantom for radiotherapy QA

[1]Alzahrani M, [2]Johnstone E, [3]Broadbent D, [1]Teh I, [3]Al-Qaisieh B, [4]Walker A, [4]Lamb R, [4]Trowell L [3]Speight R

[1]Leeds Institute of Cardiovascular and Metabolic Medicine, University of Leeds, UK.
[2]Christie Medical Physics and Engineering, The Christie NHS Foundation Trust, UK.
[3]Department of Medical Physics and Engineering, Leeds teaching Hospitals NHS Trust, UK.
[4]Leeds Test Object, UK.

Background. Recently, interest in magnetic resonance imaging (MRI) in radiotherapy (RT) has increased. Multimodal anthropomorphic phantoms offer a tool with a known ground truth for quality assurance (QA) of MRI for RT [1].

Methods. An outer shell and internal bone structure were 3D printed using segmented computed tomography (CT) data. Polyvinyl alcohol cryogel solution was chosen as a brain surrogate material. The remainder of the phantom was filled with deionized water. A superior region has been designed that can accommodate a dosimeter. The brain CT and MRI properties in the phantom have been measured over time to assess its stability

Results. Figure 1 shows CT, MRI images, and T1 and T2 maps of the phantom. Figure 2 shows the CT number, T1 and T2 relaxation time of the brain over time in comparison with literature values [2].

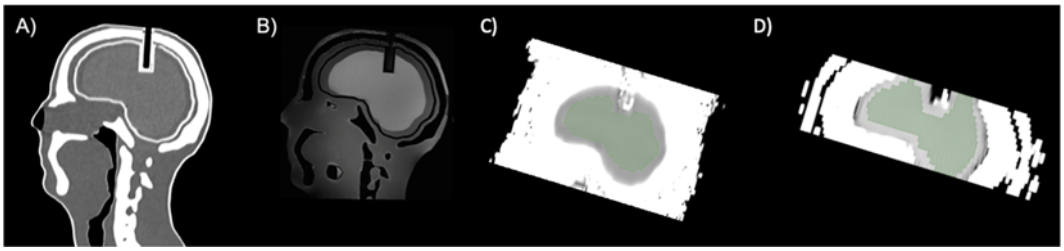

Figure 1. Sagittal CT (A) and T2-FLAIR (fluid-attenuated inversion recovery) MRI (B) images of the phantom. At the top of the head, a space was designed to allow the placement of a dosimeter. Sagittal T1 map (C) and T2 map (D) showing the ROIs (green area) in which the MRI relaxation times were measured.

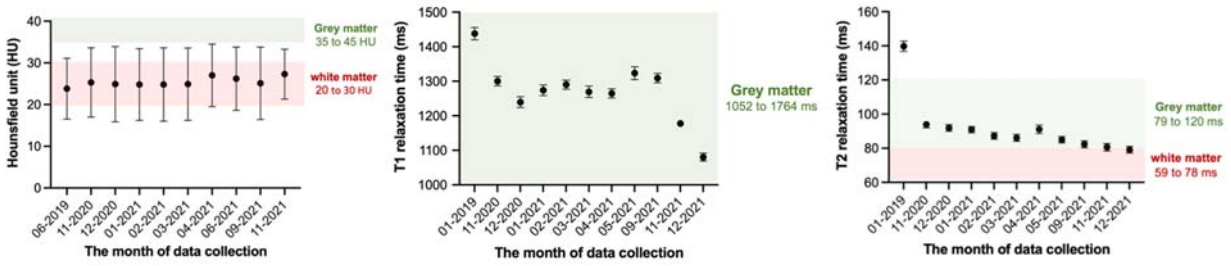

Figure 2. Hounsfield units, T1 and T2 relaxation times measured in the brain of the phantom over time. The mean (circles) and standard deviation (error bars) are displayed.

Discussion. Except for the first measurement of the T2 relaxation time, the brain CT number, T1 and T2 relaxation times appear to be appropriate for simulating the human brain. There was a notable change in MRI relaxation times between the first and second measurements and further study is needed to assess when this change occurred. An ongoing project is looking at the utility of this phantom in QA for MRI in RT, as well as evaluating further potential tissue-equivalent materials for their stability with dose and time.

Conclusion. A phantom has been developed that mimic the human head and neck in both MRI and CT imaging. CT numbers in the brain appear to be stable over time. However, there appears to be a noticeable change in MRI relaxation times that needs further investigation.

Key references.

1. Speight, R, et al. 2021, *Physics in Medicine & Biology,* **66**(5), p.055025.
2. Bojorquez, J. Z, et al. 2017 *Magnetic resonance imaging,* **35**, pp.69-80.

Comprehensive Dose Evaluation of Synthetic CT for Pelvic MR-only Radiotherapy

[1,2]Wyatt J, [3]Kaushik S, [3]Cozzini C, [3]Wiesinger F, [1,2]Pearson R, [1]Maxwell R, [1,2]McCallum H,
[1]Translational and Clinical Research Institute, Newcastle University, UK.
[2]Northern Centre for Cancer Care, Newcastle upon Tyne Hospitals NHS Foundation Trust, UK.
[3]GE Healthcare, Munich, Germany

Background. Radiotherapy is an essential treatment for patients with pelvic cancers[1]. Magnetic Resonance (MR) -only radiotherapy enables the superior soft-tissue contrast of MR to be used without the uncertainty of a MR- Computed Tomography (CT) registration[2]. This requires a method of generating a synthetic CT (sCT) from the MR for radiotherapy dose calculations[3]. The primary challenge for sCT is distinguishing bone from air[4]. A novel Zero Echo Time (ZTE) sequence enables signal from the bone to be captured[5]. This study aimed to evaluate for all pelvic radiotherapy sites a Deep Learning (DL) sCT algorithm based on the ZTE sequence.

Methods. ZTE images of 33 pelvic radiotherapy patients (6 female, 27 male) were acquired in the radiotherapy position within one week of the planning CT. A DL sCT algorithm was trained using paired data from the ZTE and deformably registered CT, using a multi-task segmentation-regression convolutional neural network with an enhanced focus on accurate bone value estimation. CTs were generated from ZTE images of a further 20 patients (14 male, 6 male), rigidly registered to the CT, with any air over-ridden to water density. A volumetric modulated arc therapy plan was optimised on CT to irradiate a cylindrical Planning Target Volume (PTV) with 10 cm diameter and 5 cm length centred between the femoral heads (FH). The plan was recalculated on sCT and difference in D50% calculated. This was repeated for PTVs centred 5 cm inferior (FH-5), 5cm (FH+5) and 10cm (FH+10) superior to FH. Points on patients with CTs that extended < 2 cm longitudinally from the PTV edge were excluded. The analysis for all points was repeated using the intersection of the sCT and CT external contours as the external contour for both images, removing dose differences in the external contours from setup differences.

Results. Example ZTE (left) and sCT (right) images are shown. D50% differences (sCT – CT) are given in the table as mean ± standard error, minimum, maximum. Within the external contour there were two patients with differences > 2% at the FH-5 point, and one patient at the FH and FH+5 points. Within the intersection contour only one patient was > 1% (for FH point).

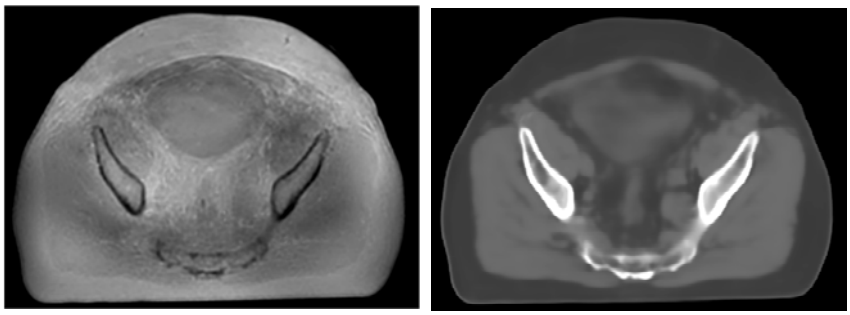

Point	Patients	Mean D50% Difference / %	
		True External	*Intersection External*
FH+10	12	-0.1 ± 0.1 $(-1.0,0.4)$	-0.3 ± 0.1 $(-0.7,0.1)$
FH+5	20	0.2 ± 0.2 $(-1.1,2.3)$	-0.1 ± 0.1 $(-0.9,0.7)$
FH	20	0.4 ± 0.2 $(-1.6,2.1)$	-0.1 ± 0.1 $(-1.2,0.6)$
FH-5	19	0.8 ± 0.2 $(-1.2,3.1)$	0.1 ± 0.1 $(-0.7,0.6)$

Discussion. Mean dose differences within the true external were ≤ 0.8% and intersection external ≤ 0.3% over all points, indicating high dose accuracy for the whole pelvis. Although there were two patients with differences > 2% within the external contour, the fact that all differences within the intersection contours were ≤ 1.2%, suggests the larger dose differences in the true external were due to setup differences rather than incorrect Hounsfield Units. Differences were largest for the FH-5 point, likely due to discrepancies in femur angle between MR and CT.

Conclusion. A DL sCT algorithm based on a novel ZTE sequence has been successfully developed for pelvic radiotherapy patients. The sCT had high dose accuracy at multiple points within the pelvis, with all D50% differences within the intersection contour ≤ 1.2% implying accurate Hounsfield Unit assignment. This suggests this sCT algorithm can enable MR-only radiotherapy for all pelvic cancers with high dose accuracy.

Key references. [2] D Bird et al., Int J. Radiat. Oncol. Biol. Phys., 105(3), 2019. [4] J Edmund et al., Radiat. Oncol., 12(1), 2017. [3] E Johnstone et al., Int J. Radiat. Oncol. Biol. Phys., 100(1), 2018. [1] K Morris et al., World J. Gastrointest. Surg., 7(11), 2015. [5] F Wiesinger et al., Magn. Reson. Med., 80(4), 2018.

Comparison of synthetic CT solutions for MR-Only VMAT prostate planning

[1]Manley, Steve
[1]Northern Centre for Cancer Care (NCCC), Freeman Hospital, Newcastle-upon-Tyne Hospitals NHS Foundation Trust

Invited talk submission

Overview of Talk:

An MR-only pathway utilises a synthetic CT (sCT) created from MRI data, obviating the need for an additional planning CT for dose calculation, with MRI providing a single dataset with increased soft tissue contrast.

Currently the NCCC use MRI Planner v2.3, a Software As A Service solution by Spectronic Medical, for MR-only planning of VMAT prostate radiotherapy. This requires patient data to be encrypted and sent offsite for processing into an sCT. Previous studies demonstrated this solution to be satisfactory for our clinical needs.

A comparable sCT feature was subsequently procured from Siemens with our new MR scanner, meaning all data would stay onsite, with only the one-off capital outlay.

This presentation will review the assessment of the Siemens solution against the prior investigation of the Spectronic solution. It will present the dose difference between the two sCT solutions, using doses to Regions of Interest (ROIs) from the CT-based approved treatment plans as baseline values.

Method:

An initial cohort of 10 patients treated at the NCCC had a baseline CT with comparative MR image sets being used to generate both sCT solutions. In all cases the clinical CT dataset was used as a baseline for dose calculation along with the clinically approved 60Gy/20 fraction VMAT plan, using RayStation V9B as the Treatment Planning Software.

The HU to electron density table provided by Siemens for the sCT required tuning, mirroring the work of Cabana et al, with subsequent in-house refinement until deemed clinically acceptable.

ROIs were copied from the CT dataset onto the sCT datasets via rigid registration for comparative dose evaluation. DVH data were extracted from RayStation for all ROI's including all Organs at Risk (OAR) and Target Volumes (TV). For all ROIs the integrated ROI dose normalised to ROI volume was used for dose difference evaluation.

Results:

Final HU conversion tables provided mean differences of individual OARs and TVs (bladder, bowel, femoral heads, prostate, seminal vesicles etc.,) of less than 0.5% from the CT baseline dose for the Siemens solution, comparable to the Spectronics solution.

Discussion / Future work:

Rigid registration led to some of the ROIs not matching exactly and would account for some discrepancy, especially in highly motile regions such as bladder and bowel etc., time between CT and MR also changed the SSD used for skin (external) ROI doses.

An issue with the Siemens solution incorrectly reconstructing the right femoral head was discovered in a small sample of cases and was further investigated through an additional cohort of 12 patient image sets processed only through the Siemens sCT solution. Resolution of this mis-placed femoral head component is still ongoing with Siemens.

MRI –RT Simulator Commissioning for Clinical and Research Radiotherapy

Marimuthu Sankaralingam[1,2], Stefanie Thomson[1,2], Martin Glegg[1,2],Sharon Cave[3], Sarah Allwood Spiers[2],John Foster[2]
Radiotherapy Physics[1] , Department of Clinical Physics & Bioengineering[2] , Radiography[3]
Beatson West of Scotland Cancer Centre,
NHS Greater Glasgow &Clyde, Glasgow

Introduction

With the increasing number of diagnostic MRI scanner installations globally, the integration of magnetic resonance imaging (MRI) into normal planning processes in radiotherapy is no longer a research endeavour. The installation, commissioning, and validation of an MRI RT simulator system are significantly different from those of a regular diagnostic MRI scanner, requiring particular attention to reproducible patient positioning and geometric accuracy, and are also dependent on the static magnetic field strength. The purpose of this presentation is to highlight the commissioning and quality assurance (QA) of Scotland's first dedicated wide-bore 1.5 Tesla (1.5T) MRI radiotherapy planning simulator.

Materials and Methods

The new Siemens Magnetom Sola RT Pro 1.5T MRI-RT simulator installation at the Beatson West of Scotland Cancer Centre (BWOSCC) began in September 2021, with the first clinical radiotherapy patient expected to be scanned in the end of March 2022. A detailed commissioning program was devised and implemented, emphasising radiotherapy (RT)-specific criteria, following advice contained in current AAPM, ACR and IPEM guidance.

The following RT-specific tests were performed: radiofrequency (RF) coil homogeneity characteristics, image quality, geometric distortion, laser and couch movement, and an end-to-end radiotherapy treatment planning test. Additionally, general system performance and safety testing were performed.
The ACR MR phantom was used to perform a number of image quality tests, with the phantom images analysed using the AutoQA Plus MR ACR program. Geometric distortion measurements are critical for radiotherapy planning and were performed using the Quasar MRID3D phantom and software. Daily image quality, laser position, and geometry checks were completed utilising an in-house flood cylindrical and Lap quality assurance phantom. In the instance of DWI QA, an in-house phantom was used to verify the ADC value's consistency. We will most likely employ the CaliberMRI Diffusion phantom in the future since it eliminates the necessity for ice cubes to regulate the temperature. Furthermore, a cylindrical phantom based on a previous work (Phys.Med.Biol.59(2014)2235-2248) was developed to evaluate fat suppression techniques and sequence optimization.4DMRI will be commissioned in the coming months using our new Quasar 4DMRI phantom; following that, 4DMRI sequences will be optimised for various clinical sites. Finally, we will establish a 4DMRI quality assurance system that will be identical to our 4DCT quality assurance regime. MRI safety governance is provided within the existing diagnostic radiology MRI safety structure. MRI safety documentation such as screening checklists and local rules were adjusted to meet the needs of the radiotherapy department.

Results and conclusion

This talk will discuss the challenges associated with installing a dedicated 1.5T MRI RT simulator in a radiotherapy department. The emphasis will be on commissioning and validation of the MRI RT Simulator and Quality Assurance software, as well as the establishment of a quality assurance regime and MRI safety. Additionally, sequence optimisation will be presented for radiotherapy planning and research radiotherapy.

Developing radiographer competencies to work in radiotherapy MR services

McDaid L[1], Doherty W[1], Hutton M[2], Clough A[1], Benson R[1], Eccles CL[1,]
[1]Department of Radiotherapy, The Christie, Manchester, UK
[2]Medical Physics and Engineering, The Christie, Manchester, UK

Background: MRI scanners housed in radiotherapy (RT) departments and integrated MR Linacs are still fairly novel(1,2). A competency-based educational framework needed to be developed to ensure that radiographers have the requisite knowledge, skills and capability to deliver safe, patient-focused MR- guided radiotherapy services.

Methods: It was determined that a hub and spoke model would be an appropriate framework. A central, or "hub", competency was developed initially and peer reviewed by identified subject matter experts (SME). Role and competency-specific spokes emanate from this central hub and were developed subsequently, with spokes identified as containing the most new knowledge being developed first. A spiral curriculum was utilised to consolidate and build on prior learning whilst introducing new topics. Trainer and assessor guides were developed to ensure standardisation of training and assessment. Learning material was validated with new staff rotating into the team and feedback used to develop and improve content and activities. Spoke competencies were developed sequentially and feedback used from one to streamline development of the next.

Results: The completed model is shown here:

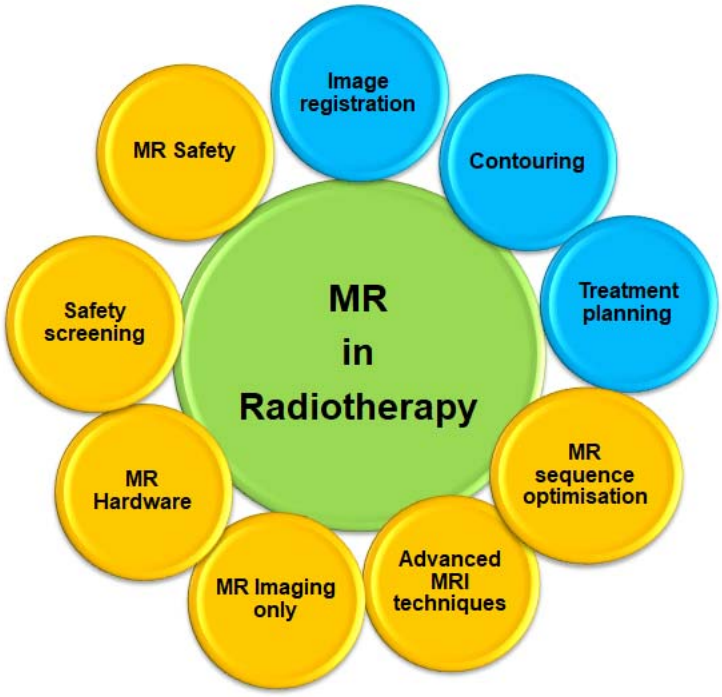

Legend: *Yellow = MRI spoke competencies which are universal across the radiotherapy services. Blue = MR Linac specific spoke competencies. Green = Hub competency.*

Conclusion: We have developed a comprehensive framework for MRI-guided RT at our institution, in the absence of a nationally provided one. The key benefit of this model is its flexibility to ensure that partial completion evidences that radiographers can perform specific roles within an MRI team and will help facilitate workforce role-mapping. We continue to seek consensus with other centres and professional bodies so that others may benefit from our preliminary work.

Key references:

1. McDaid L, Hutton M, Cooper L, Hales RB, Parry C, Waters J, et al. Developing electronic learning to deliver MR safety training in a radiotherapy department. J Med Imaging Radiat Sci [Internet]. 2021;52(4):S24–31. Available from: https://doi.org/10.1016/j.jmir.2021.05.012
2. Speight R, Schmidt MA, Liney GP, Johnstone RI, Eccles CL, Dubec M, et al. IPEM Topical Report: A 2018 IPEM survey of MRI use for external beam radiotherapy treatment planning in the UK. Phys Med Biol [Internet]. 2019 5;64(17):175021. Available from: http://dx.doi.org/10.1088/1361-6560/ab2c7c

Perfusion MRI in evaluation of brain metastases: current practice and rationale for baseline MR perfusion imaging prior to stereotactic radiosurgery (a feasibility study)

[1]Dobeson C, [2]Birkbeck M, [1]West S, [3]Bhatnagar P, [3]Hall J, [1]Lewis J
[1]Department of Oncology, Northern Centre for Cancer Care, Freeman Hospital, Newcastle upon Tyne, UK. [2]Northern Medical Physics and Clinical Engineering, Freeman Hospital, Newcastle upon Tyne, UK. [3]Department of Neuroradiology, Royal Victoria Infirmary, Newcastle upon Tyne, UK.

Background

Stereotactic radiosurgery (SRS) is an established focal treatment for brain metastases with local control rates of 75-90% at 1 year (1). An important side-effect of SRS is the development of radionecrosis – cerebral tissue damage due to radiation. Radionecrosis and tumour progression often have similar appearances on conventional MR imaging, but have different management approaches. Perfusion MR is relied upon in gliomata to help distinguish between the two, however, interpretation of perfusion MR in the post-treatment metasteses setting is complex. The STARBEAM-X study (Study of assessment of radionecrosis in brain metastases using MR perfusion imaging) has been designed with the aim of assessing the clinical application of baseline MR perfusion imaging prior to SRS as part of the radiotherapy planning process. We hypothesise that baseline perfusion imaging will aid post-treatment imaging interpretation by enhancing our understanding of how a metastesis perfusion characteristics change after treatment with SRS.

Methods

Baseline perfusion MR imaging has been performed on 3 patients to assess feasibility. Perfusion data were acquired on a Siemens Magnetom Sola 1.5T scanner. Scan parameters were: Field of view=230x230mm, in-plane resolution=1.8x1.8mm, slice thickness=5mm, TE/TR=31/1920ms. Scans were acquired during a bolus injection of gadovist contrast agent over 60 phases. Total acquisition time=2 minutes. The MRI protocol including pre and post contrast sequences was 30 minutes in duration. Relative Cerebral Blood Volume (rCBV) perfusion maps were calculated in Syngo.Via software and interpretation performed by an expert Neuroradiologist.

Results

Example perfusion maps from one patient are shown in figure 1. Relative CBV was successfully extracted from the maps in all three patients. The addition of the perfusion MRI sequence added 2 minutes to the existing MR protocol.

Discussion

Image quality was sufficient for accurate clinical diagnosis at 1.5 T. Perfusion data was of sufficient quality to assess baseline perfusion characteristics of tumours in all patients.

Conclusion

The pilot phase of this study has demonstrated that incorporating baseline perfusion imaging into standard of care radiotherapy SRS metasteses planning MR imaging is feasible, with low associated time-burden. The study team look forward to presenting the results of STARBEAM-X in due course.

References

1. Redmond KJ et al. Tumor Control Probability of Radiosurgery and Fractionated Stereotactic Radiosurgery for Brain Metastases. Int J Radiat Oncol Biol Phys. 2021 May 1;110(1):53-67

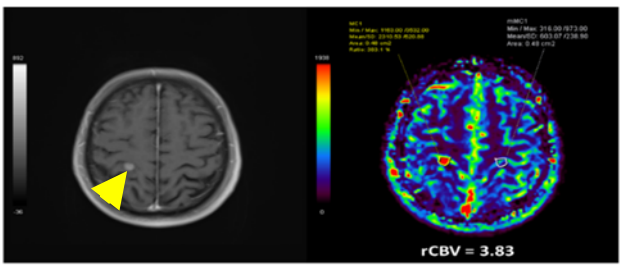

Figure 1: Left – post contrast T1w VIBE demonstrating enhancement of the lesion (yellow arrow). Right – quantitative DSC perfusion map, lesion delineated in yellow and mirrored region of interest in white. rCBV indicated below in white.

An Update on the Sheffield Stereotactic Radiosurgery Phantom – Analysis with In-House Software

[1]Goodall A, [1]Powell S, [1]Harris P, [1]Walton L, [1]Siddall, L, [1]Hunt K, [1]Fry A
[1]Sheffield Teaching Hospitals NHS Foundation Trust

Background: In 1996 and 1997 Walton et al presented two papers [1, 2] describing the development and testing of a phantom for use in assessing the accuracy of MR imaging for stereotactic radiosurgery. Since then this phantom has undergone slight modifications. Rods in the phantom create a void in the MR image and the centre of those voids is used to measure the distortion. This new phantom has been in routine use at Sheffield Teaching Hospitals (STH) for over 15 years, for testing and optimisation of stereotactic sequences at MR system installation and for subsequent annual QA on each scanner. Measurement of the distortion is usually performed manually, with clinical scientists marking the centre of each void. This is laborious work taking approximately half an hour per sequence and does not analyse all of points on all of the slices.

Methods: Recently, a software application has been developed in ImageJ (ImageJ 1.53i, National Institutes of Health, USA, http://imagej.nih.gov/ij) that performs an automated analysis of the images allowing all of the voids on all of the slices to be analysed with minimal user input. The phantom was scanned with a range of clinical MR sequences used for stereotactic radiosurgery, brachytherapy and radiotherapy treatment planning. The software was used to analyse the distortion present on these images and the results compared to those from a manual assessment.

Results: When run on a series of synthetic test images with known distortions ranging from -3 mm to + 3mm in both x and y directions, Bland-Altman plots[3] showed that the software had a bias of less than 0.02 mm compared to the set value. Testing of sequences used for stereotactic radiosurgery, brachytherapy and radiotherapy treatment planning has been performed and shows that the mean distortion in all directions in-plane is less than 0.5 mm with the maximum distortion not exceeding 2 mm as per the recommended guidance[4, 5]. The time to analyse each image set was 2.1 +/- 0.9 minutes - much less than the 30 minutes required for a manual measurement. Comparisons to manual measurements showed a bias, (manual – automated) of just -0.03 mm for the mean values, and -0.36 mm for the maximum values.

Discussion: Over 1400 voids per sequence were analysed which would take considerable time for a person to do manually, and provides a more comprehensive picture of the distortion present in the sequence. There is a small bias in the software; however, this is far below the pixel size of the images and so is negligible. Compared to manual measurements, the mean values also had a negligible bias. The maximum distortion was slightly larger as manual testing did not measure the voids at the corners of the phantom which are likely more distorted. The increased speed of the analysis makes this ideal for making comparisons between sequences after optimisation or any minor scanner issues or software upgrades. Currently, there is no way to add the data into the stereotactic radiosurgery treatment planning software, and so some manual measurements will need to continue.

Conclusion: The automated software allows for quick and comprehensive analysis of the distortion in an MR image. The results are comparable to those made manually and show a negligible bias compared to known distortion values. This will save valuable time for clinical scientists.

Key references.

1. Walton L, Hampshire A, Forster D, Kemeny A – A Phantom Study to Assess the Accuracy of Stereotactic Localization, Using T1-weighted MRI with Leksell Stereotactic System - Neurosurgery, 38: 170-8, 1996
2. Walton L, Hampshire A, Forster D, Kemeny A – Stereotactic Localization with MRI: A Phantom Study to Compare the Accuracy Obtained Using Two-dimensional and Three-dimensional Data Acquisitions - Neurosurgery 41: 131-9, 1997
3. Giavarina D. Understanding Bland Altman analysis. Biochem Med (Zagreb). 2015;25(2):141-151. Published 2015 Jun 5. doi:10.11613/BM.2015.015
4. Greener A. - Practical Determination of Systematic and Random set-up error using portal imaging – Geometric Uncertainties In Radiotherapy, London: BIR, 2003: 36-43
5. Harrison A, McKenzie A – Standard Deviation of a top-hat function – Geometric Uncertainties In Radiotherapy, London: BIR, 2003: Appendix 2b

Title of Study: Development of a Virtual Three-Dimensional MRI Distortion Characterisation Phantom

[1,2]Telfer SA, [1,2]Phillips J
[1]Medical Physics and Clinical Engineering, Swansea Bay University Health Board, UK.
[2]Medical School, Swansea University, UK.

Background: The use of magnetic resonance imaging (MRI) and its superior tissue contrast in radiotherapy pathways is constrained by geometric distortion [1, 2]. To meet enhanced quality assurance needs, researchers and manufacturers have developed 3D geometric assessment phantoms that use control points (CPs) formed by either 1) intersecting orthogonal planes such as the grid–based phantom introduced by Wang *et al* [3,6-8] or 2) spherical objects as in Phillips [4], GE Healthcare prototype [5] and Spectronic phantoms [9]. A versatile 3D geometric distortion grid phantom that extends the features of the original Wang phantom has been designed by J. Phillips. The main aims of this project were to virtually develop and perform initial evaluation of the phantom design using realistic simulated MR images created in Matlab.

Methods: In the phantom, CPs in each plane are formed by intersecting orthogonal planes arranged in a "nested" grid pattern. Multiple grids can be stacked together to evaluate large image volumes. A Matlab function utilising methods of generating geometrical objects in 3D arrays was developed to create the virtual phantom with specified dimensions, see fig. 1a). Further development investigated creating realistic simulated MR images of the phantom with different slice profiles, random intensity fluctuations, and distortion, which can be controlled by specified variables such as a factor that adjusts Gaussian slice profiles, signal-to-noise ratio controlling Gaussian probability distributions, and coefficients in series expansions of r in spherical coordinates image transforms, respectively.
Initial analysis of simulated perfect and distorted single slice images from each plane applied methods from Wang *et al* [7,8]. CP locations are enhanced by determining first derivatives in each plane followed by convolution with cross-like masks, see fig. 1b). Reference locations of the CPs can be extracted using orthogonal intensity profiles. Analysis was extended for all axial CPs in the perfect simulated image volume. The reference locations form the centre of small sampling volumes where the first moments are calculated in each plane in the gradient images, subsequently providing an estimate of the CP locations.

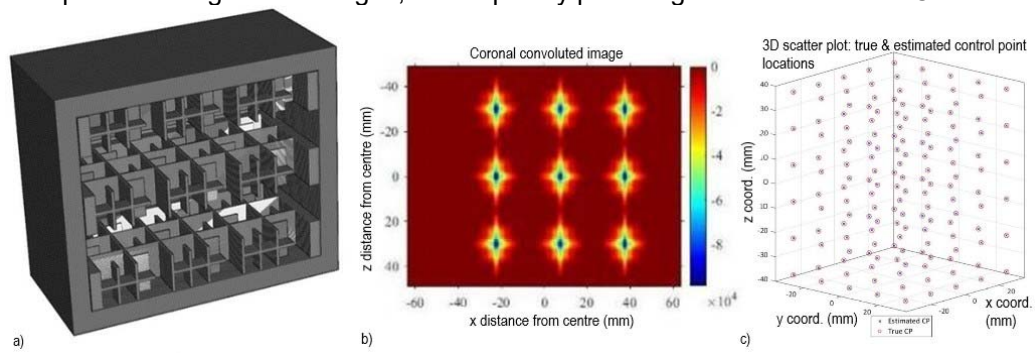

Figure 1: a) cross-section virtual grid phantom with additional CPs in sagittal and coronal planes, b) coronal convoluted image, c) estimated and true axial CP locations.

Results: In the initial analysis, reference locations for each plane were found to be located within ≤±½ pixels (*x, y* coordinates) and ≤1 pixel (*z* coordinates) of the theoretical control point locations in the image volume. The estimated axial control point locations were found to exactly match theoretical control point locations in the virtual image volume, see fig 1c).

Discussion/Conclusion: Initial results demonstrate that Wang's methods can be successfully applied in each phantom plane to enhance features and extract reference locations close to theoretical locations, and accurately estimate axial control point locations in image volumes. Therefore, the feasibility of using the phantom design, which provides increased control point density for evaluating geometric distortion and gradient performance in three orthogonal planes in one image acquisition has been demonstrated. Use of a virtual phantom allows design evaluation, and enables development and robust testing of control point detection algorithms before manufacture, reducing costs.

Key references. In alphabetical order, numbered.

1. Baldwin LN *et al*. A two-step scheme for distortion rectification of magnetic resonance images. Medical Physics. 2009; 36: 3917-26.
2. Chin S, *et al*. Magnetic resonance-guided radiation therapy: A review. Journal of Medical Imaging and Radiation Oncology. 2020;64: 163-77.
3. Shan S, *et al*. Geometric distortion characterization and correction for the 1.0 T Australian MRI-Linac system using an inverse electromagnetic method. Medical Physics. 2020; 47, 1126-38.
4. Tijssen RHN *et al*. MRI commissioning of 1.5T MR-Linac systems – a multi-institutional study. Radiotherapy and Oncology. 2019; 132: 114-20.
5. Torfeh T *et al*. Characterization of 3D geometric distortion of magnetic resonance imaging scanners commissioned for radiation therapy planning. Magnetic Resonance Imaging. 2016; 34: 645-53.
6. Wang D *et al*. A proposed scheme for comprehensive characterization of the measured geometric distortion in magnetic resonance imaging using a three-dimensional phantom. Medical Physics. 2004; 31: 2212-18.
7. Wang D *et al*. A novel phantom and method for comprehensive 3-dimensional measurement and correction of geometric distortion in magnetic resonance imaging. *Magnetic Resonance Imaging*. 2004; 22: 529-42.
8. Wang D *et al*. Geometric distortion in clinical MRI systems Part I: evaluation using a 3D phantom. *Magnetic Resonance Imaging*. 2004; 22: 1211-21.
9. Wyatt J *et al*. Evaluating the repeatability and set-up sensitivity of a large field of view distortion phantom and software for magnetic resonance-only radiotherapy. Physics and Imaging in Radiation Oncology. 2018; 6: 31-8.